

Instabilities of switching processes in synthetic antiferromagnets

A. N. Bogdanov and U. K. Rössler[†]

IFW Dresden, Postfach 270116 D-01171 Dresden, Germany

(Dated: December 21, 2021)

It is shown that magnetic states and field-driven reorientation transitions in synthetic antiferromagnets crucially depend on contributions of higher-order anisotropies. A phenomenological macrospin model is derived to describe the magnetic states of two antiferromagnetically coupled magnetic thin film elements. The calculated phase diagrams show that magnetic states with out-of-plane magnetization, symmetric escaped spin-*up* phases, exist in a broad range of the applied magnetic field. Due to the formation of such states and concomitant multidomain patterns, the switching processes in toggle magnetic random access memory devices (MRAM) can radically deviate from predictions within oversimplified models.

PACS numbers: 75.70.Cn, 75.50.Ee, 75.30.Kz, 85.70.Li,

Recently, a controlled switching of synthetic antiferromagnetic thin film elements has received high interest as active part of so-called toggle magnetic random access memory systems [1]. In these devices, an antiferromagnetically coupled two-layer system undergoes a field-driven reorientation. Various intrinsic and induced magnetic couplings in nanomagnetic layer systems lead to complex magnetic behaviour characterized by an unusually large number of magnetic states and transitions between them (see, e.g., [2]). Therefore, even simplified phenomenological single-domain (or macro-spin) models display a great many magnetic states and complex magnetization processes [3, 4]. However, a general analysis can be given in terms of the topologically different types of magnetic phase diagrams to identify the stability of magnetic states with respect to different perturbing interactions and the occurrence of metastable states.

In this Letter, we show that higher-order anisotropies give rise to additional magnetic states with out-of-plane magnetization in synthetic antiferromagnets. Qualitatively, this effect is easily understood. The field-driven reorientation transition in a synthetic two-layer antiferromagnet with a common uniaxial anisotropy is akin to the spin-*up* transition in a classical two-sublattice antiferromagnet. At the spin-*up* field, the uniaxial anisotropy and the Zeeman energy balance each other. Hence, near the spin-*up* field, the magnetic state is subject to weaker higher-order anisotropies. This may cause magnetic instabilities. Here, we analyse the instability mechanism for an elementary macrospin model with competing uniaxial and cubic anisotropy. This model is relevant for many magnetic layer systems with an intrinsic cubic magnetocrystalline anisotropy and an in-plane easy axis, e.g. induced by substrate-film interactions. However, such instabilities of the spin-*up* phase in an antiferromagnet

are a general phenomenon related to higher-order magnetic anisotropies. E.g., a spin-*up* phase transverse to the easy axis and an obliquely applied field can also be stabilized by (intrinsic or induced) fourth order uniaxial anisotropy, as has been observed and analysed quite a long time ago for bulk Cr [5]. Similar escaped spin-*up* states arise due to a secondary easy axis. In layered synthetic antiferromagnets, such a biaxial anisotropy can be induced by perpendicular surface anisotropy of the single ferromagnetic layers [6, 7, 8].

We consider spatially homogeneous states in two physically identical ferromagnetic layers with a circular cross section (or infinite in the basal plane) and an exchange-coupling through an interlayer. The phenomenological energy for this two-layer system can be written as [2]

$$W = J m_1 \cdot m_2 - J h \cdot (m_1 + m_2) + \sum_{i=1}^2 W_a^{(i)}; \quad (1)$$

where the unity macrospins $m_i = \langle M_i \rangle / M_0$ point along the average of the magnetization distribution M_i , which is given by $\langle M_i \rangle = \int M_i d^3 r_i$, $M_0 = \int m_i d^3 r_i$ for the i th layer with volume V_i . The effective interlayer exchange is antiferromagnetic, $J = M_0^2 \int m_1(r_1; r_2) d^3 r_1 d^3 r_2 > 0$. In the Zeeman term, the reduced (internal) field $h = H = H_e$ with $H_e = J/M_0$ comprises applied and stray fields. The magnetic anisotropies should also be considered as volume averages $W_a^{(i)} = \int w_i d^3 r_i$. The form of energy (1) coincides with the (mean-field) energy of a bulk two-sublattice antiferromagnet with "sublattice magnetizations" m_i (see review and bibliography in [9, 10]). The magnetic anisotropy of our model considers a uniaxial (K) and a cubic (K_c) contribution $W_a^{(i)} = K(m_i \cdot \hat{n})^2 + K_c[(m_i \cdot \hat{x})^4 + (m_i \cdot \hat{y})^4 + (m_i \cdot \hat{z})^4] = 4$.

By a standard procedure we introduce the vector of the total magnetization $M = m_1 + m_2$ and the staggered vector $L = m_1 - m_2$. Because $\int m_i d^3 r_i = 1$, the following constraints hold: $M \cdot L = 0$ and $M^2 + L^2 = 1$. For weak anisotropy $J \ll K; K_c$ the magnetic energy Eq. (1) can be simplified as $W = J(2M^2 - 1) - 2Jh \cdot M + K[(1 - L^2)(1 - \hat{n}^2) + (M \cdot \hat{n})^2] + K_c[(1 - \hat{x})^4 + (1 - \hat{y})^4 + (1 - \hat{z})^4] = 2$,

Permanent address: Donetsk Institute for Physics and Technology, 340114 Donetsk, Ukraine; Electronic address: bogdanov@ifw-dresden.de

[†]Corresponding author; Electronic address: u.roessler@ifw-dresden.de

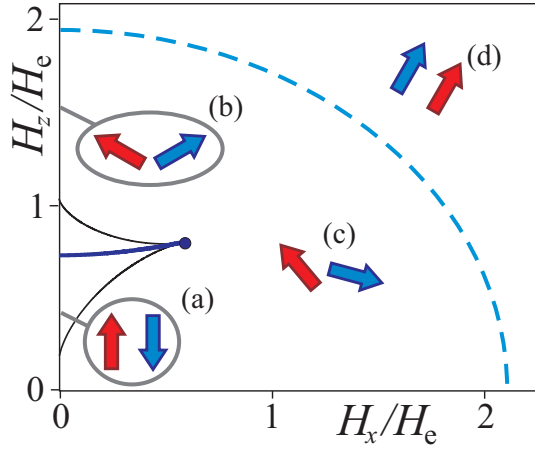


FIG. 1: The magnetic phase diagram for small cubic anisotropies $K_c < K$ holds only planar stable phases. Antiferromagnetic (a) and spin-flop (b) states exist in a magnetic field H_z along the easy axis n . The first-order (spin-flop) transition occurs in the critical field h_{SF} . In oblique magnetic fields, $H_x \neq 0$, the transition occurs between canted (c) phases that are distorted antiferromagnetic and spin-flop states. Stability limits of metastable states are given by thin lines. Dashed line gives the continuous transition into the spin-flop (saturated ferromagnetic) phase.

where $l = L = \sum_j j$ is the unity vector along the staggered vector. An independent minimization with respect to M yields $M = [h - (h - l)]/2$ (for details, see similar calculations in bulk systems, e.g. [9]). After substituting this expression for M and omitting constant terms, one obtains the magnetic energy as function of the unity vector $l = (\sin \theta \cos \phi; \sin \theta \sin \phi; \cos \theta)$ as

$$\tilde{W} = (J - (K=4) \cos(2\theta)) (h^2 - 1) - K \cos^2 \theta - K_c (1 + \cos^2 2\theta - \sin^4 \theta - \sin^2 2\theta) = 4; \quad (2)$$

for a configuration with the uniaxial direction n and one of the cubic axis a_i along the Z axis, and for magnetic fields restricted to the XOZ plane, $h = (h \sin \theta; 0; h \cos \theta)$. Depending on the ratio between uniaxial and cubic anisotropy, there are three topologically different magnetic phase diagrams.

I. For $K > K_c$ only planar phases with $\theta = 0$ are stable, i.e., the magnetization vectors are in XOZ plane. In this case energy (2) can be reduced to the following functional

$$\tilde{W}(\phi) = \frac{\mathcal{H}}{2} \cos^2 2\phi - \mathcal{H}_z \cos 2\phi - \mathcal{H}_x \sin 2\phi; \quad (3)$$

where $\mathcal{H} = K h^2 + 2K_c$, $\mathcal{H}_z = \frac{J}{2} h^2 \cos 2\theta - h_{SF}^2$, $\mathcal{H}_x = J h^2 \sin 2\theta$, and $h_{SF} = \frac{J}{2K} = \frac{J}{2K_c}$ is the reduced spin-flop field.

The energy (3) is akin to the free energy of a bulk uniaxial ferromagnet [11] and of antiferromagnets [10]. The corresponding magnetic phase diagram is shown in Fig. 1. At zero field and in a magnetic field along the Z axis,

$h < h_{SF}$, the antiferromagnetic phase (Fig. 1 (a)) has the lowest energy while the spin-flop phase ($l \parallel x$ axis, Fig. 1 (b)), has lowest energy for $h_{SF} < h < h_1 = 2 - K_c/J = 2 - K_c/K$. At the field h_{SF} a proper spin-flop takes place. This is the first-order transition between the collinear and the flopped states. As the field approaches h_1 the spin-flop phase continuously transforms into the saturated spin-flop phase, Fig. 1 (c). In magnetic fields with components transverse to the easy direction, a canted phase is stable, Fig. 1 (d). The region of the metastable states near the spin-flop transition is circumscribed by a modified astroid $(\mathcal{H}_x)^{2/3} + (\mathcal{H}_z)^{2/3} = (\mathcal{H})^{2/3}$. The hyperbola $h^2 \cos 2\theta = h_{SF}^2$ gives the line of the first-order transition between the distorted antiferromagnetic phase, $\theta_1 = \arcsin(\tan 2\theta = \tan 2\theta_c) = 2$, and the spin-flop phase, $\theta = 2$, where the maximum angle $\theta_c = \arctan(K = J + K_c = K) = 2$ designates the end point of the first-order transition line, Fig. 1.

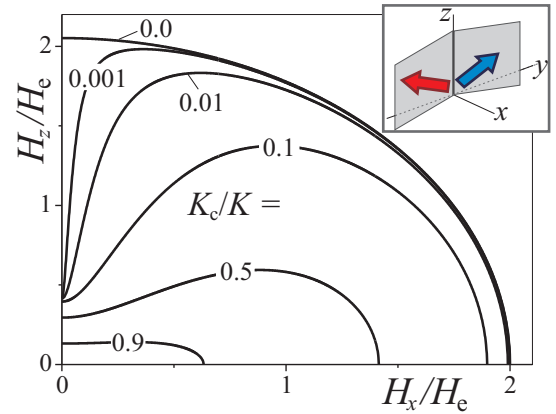


FIG. 2: Stability lines of the escaped spin-flop phase for $K=J=0.1$ and different ratios between cubic and uniaxial anisotropy.

In a purely uniaxial system, ($K_c = 0$), the spin-flop state has an infinite degeneracy with respect to rotation of the vector l around the Z axis. Application of a magnetic field with a component transverse to the easy axis lifts this degeneracy. Then only a canted phase exists with the magnetization vectors in the plane spanned by the easy direction and H (the XOZ) plane in Fig. 1).

A remarkably different situation occurs for nonzero K_c . The cubic anisotropy reduces the degeneracy of the spin-flop phase to two preferable directions in the XOY -plane, a_x and a_y in our model. For finite K_c , a small enough component of the magnetic field along the X axis can not destroy the local stability of the spin-flop configurations with $l \parallel y$. This implies that cubic anisotropy can stabilize spin-flop states with magnetization components out of the plane, which we call a symmetric escaped spin-flop state.

In the limit of weak anisotropies the escaped spin-flop

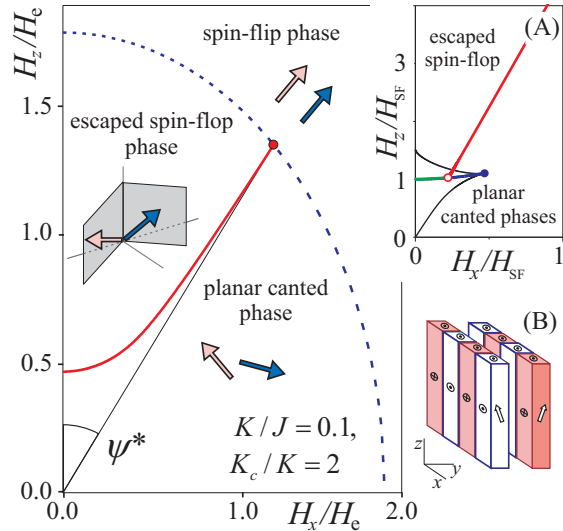


FIG. 3: The magnetic phase diagram for $K < 3K_c=4$ contains a first order transition, thick (red) line, between the canted and escaped spin-flop phase. Both phases continuously transform into the saturated state at critical lines (dashed blue). The first-order and two second-order lines meet in a bicritical point. Inset (A): the phase diagram for case $K_c > K > 3K_c=4$, is intermediate between the simple case planar $K > K_c$ and the main figure. Inset (B): sketch of a multidomain pattern in the escaped spin-flop phase.

configuration can be written as

$$m_1(m_2) = (h \sin(\theta) = 2; \quad (\theta) = \arctan\left(\frac{h_z}{h_x}\right); h \cos(\theta) = 2): \quad (4)$$

Note that the escaped spin-flop configuration (4) is degenerate with respect to the sign of the y-components.

The stability line for the escaped spin-flop phase can be readily derived from Eq. (2)

$$h_z^2 = \frac{2J^2(1 - (K_c=K))}{h_x^2(2J - K) + 4(K_c=K)(2J + 3K)} : \quad (5)$$

For weak cubic anisotropy, $K_c=K \approx 1$, the stability region of the escaped phase is restricted to a narrow strip near the H_z axis and the vicinity of the spin-flop field (Fig. 2). This region gradually spreads with increasing

$K_c=K$, and for $K_c=K > 1$ it covers the whole phase plane below the spin-flop line.

II. $K_c > K > 3K_c=4$ For $K_c > K$ the escaped phase has lowest magnetic energy and, therefore, it becomes stable in certain regions of the phase diagram (Fig. 3). The first-order transition line between the escaped and canted phase, red lines in Fig. 3, is given by a set of parametric equations

$$\begin{aligned} s &= \frac{2K}{J(1 - \sin^2 \theta)} \sin^2 \theta; \\ (h_x; h_z) &= \left(\frac{2K}{J(1 - \sin^2 \theta)} \sin^2 \theta; 1 - \sin^2 \theta \right) \end{aligned} \quad (6)$$

with $\theta = K_c=K$ and the solution for the canted phase at the transition line. For $1 < K_c=K < 4=3$, the transition line between the canted and the escaped states consists of a low field line and a high field line (green and red in Fig. 3 (A)). These lines meet each other and the first-order line between two differently canted phases (blue) in a triple point $(h_x^{(tr)} = \frac{2}{J} \frac{K_c - K}{K_c - K} = \frac{2}{J} \frac{K_c - K}{K_c - K}; h_z^{(tr)} = \frac{2}{J} \frac{K_c - K}{K_c - K})$.

III. $K < 3K_c=4$. For $K_c = 4K=3$, the triple point merges with the end point of the transition between the canted phases. The topology of the phase diagram changes (Fig. 3) and now includes only one first-order transition line between the escaped and the canted planar phases. This first-order transition line (Eq.(6)) ends at a bicritical point $(h_x = \frac{2}{J} \frac{K_c - K}{K_c - K} = K_c; h_z = 2 = \frac{2}{J} \frac{K_c - K}{K_c - K})$ with $\theta = \arctan\left(\frac{K_c - K}{K_c - K}\right) = K$, where two continuous spin-flop lines meet.

The degeneracy of the escaped phases (4) with respect to the out-of-plane components of the magnetization may lead to the formation of regular multidomain states (Fig. 3 (B)). The demagnetization in these domain structures effectively counteracts the antiferromagnetic coupling.

The results for the model with a competition of uniaxial and cubic anisotropies exemplify the occurrence of escaped magnetic configurations in antiferromagnetic layer systems. The escaped phase is metastable in wide regions of the field even for weaker cubic anisotropies. Therefore, switching processes in toggle mode MRAM devices may fail because the field-driven system can escape into metastable states with perpendicular magnetization components and the ensuing strong demagnetization effects.

Acknowledgments. Work supported by DFG (RO 2238/6). A.N.B. thanks H. Eschrig for support and hospitality at IFW Dresden.

[1] T.M. Mattheis, J.K. DeBrosse, J.A. Gaboric, E.T. Gow, M.C. Lomrey, J.S. Parenteau, D.R. Willmott, M.A. Wood, W.J. Gallagher, IBM J. Res. & Dev. 50, 25 (2006).
 [2] U.K. Røler, A.N. Bogdanov, Phys. Rev. B 69, 184420 (2004).
 [3] D.C. Worledge, Appl. Phys. Lett. 84, 2847 (2004); IBM J. Res. & Dev. 50, 69 (2006).
 [4] S.-Y. Wang, H. Fujwara, J. Appl. Phys. 98, 024510

(2005); S.-Y. Wang, H. Fujwara, M. Sun, J. Appl. Phys. 99, 08N903 (2006).
 [5] Z. Barak, E. Fawcett, D. Feder, G. Lorincz, M.B. Walker, J. Phys. F: Metal Physics 11, 915 (1981).
 [6] L. Néel, J. Physique Radium 15, 225 (1954).
 [7] A.N. Bogdanov, U.K. Røler, K.-H. Müller, J. Magn. Mater. 238, 155 (2002).
 [8] A.N. Bogdanov, A.V. Zhuravlev, I.V. Zhikharev, U.K. Røler, J. Magn. Mater. 290-291, 768 (2005).

- [9] A. N. Bogdanov, U. K. Röler, M. Wolf, K. H. Müller, Phys. Rev. B **66**, 214410 (2002).
- [10] V. G. Bar'yakhtar, A. N. Bogdanov, and D. A. Yablonskii, Usp. Fiz. Nauk. **156**, 47 (1988) [Sov. Phys. Usp. **31**, 810 (1988)].
- [11] A. Hubert, R. Schäfer, Magnetic Domains (Springer-Verlag, Berlin, 1998).